Article

Electrochemical Catalysis of Styrene Epoxidation with Films of MnO Nanoparticles and HO

Laura Espinal, Steven L. Suib, and James F. Rusling

J. Am. Chem. Soc., **2004**, 126 (24), 7676-7682• DOI: 10.1021/ja048940x • Publication Date (Web): 26 May 2004

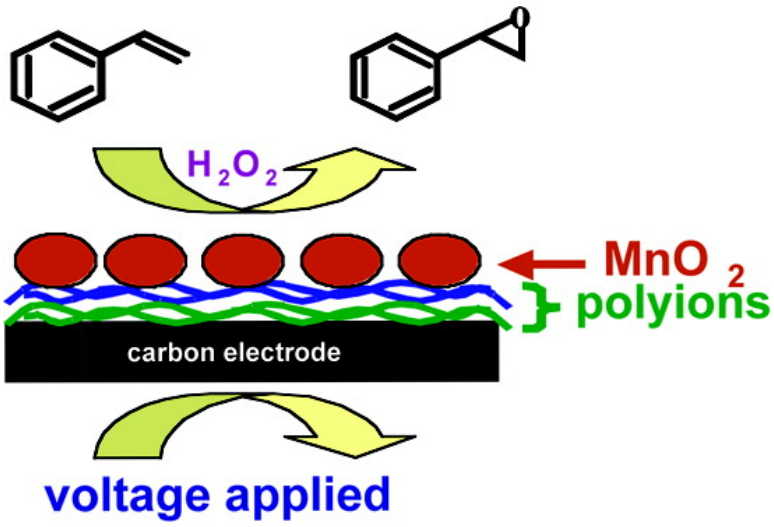

More About This Article

Additional resources and features associated with this article are available within the HTML version:

- Supporting Information
- Links to the 7 articles that cite this article, as of the time of this article download
- Access to high resolution figures
- Links to articles and content related to this article
- Copyright permission to reproduce figures and/or text from this article

View the Full Text HTML

J|A|C|S
ARTICLES
Published on Web 05/26/2004

Electrochemical Catalysis of Styrene Epoxidation with Films of MnO_2 Nanoparticles and H_2O_2

Laura Espinal,[†,§] Steven L. Suib,*[,†,‡,§] and James F. Rusling*[,†,§,||]

Contribution from the Department of Chemistry, Department of Chemical Engineering, and Institute of Materials Sciences, University of Connecticut, Storrs, Connecticut 06269-3060, and Department of Pharmacology, University of Connecticut Health Center, Farmington, Connecticut 06032

Received February 25, 2004; E-mail: steven.suib@uconn.edu; james.rusling@uconn.edu

Abstract: Films of polyions and octahedral layered manganese oxide (OL-1) nanoparticles on carbon electrodes made by layer-by-layer alternate electrostatic adsorption were active for electrochemical catalysis of styrene epoxidation in solution in the presence of hydrogen peroxide and oxygen. The highest catalytic turnover was obtained by using applied voltage −0.6 V vs SCE, O_2, and 100 mM H_2O_2. ^{18}O isotope labeling experiments suggested oxygen incorporation from three different sources: molecular oxygen, hydrogen peroxide, and/or lattice oxygen from OL-1 depending on the potential applied and the oxygen and hydrogen peroxide concentrations. Oxygen and hydrogen peroxide activate the OL-1 catalyst for the epoxidation. The pathway for styrene epoxidation in the highest yields required oxygen, hydrogen peroxide, and a reducing voltage and may involve an activated oxygen species in the OL-1 matrix.

Introduction

Epoxides are important intermediates for the manufacture of a range of modern commercial products such as epoxy resins,[1] textiles,[2] surface coatings,[1] and biological chemicals.[3] Currently epoxides are prepared from alkenes on an industrial scale using oxygen, peroxides, and peracids. Ethylene oxide is industrially obtained by gas-phase oxidation of ethylene using a supported silver catalyst in oxygen environments whereas propylene oxide is produced by metal catalyzed liquid-phase oxidation of propylene using peroxides.[4,5] Many polyoxometalate salts[6,7] and oxometallacycles[8] have been used for epoxidation as well as several homogeneous coordination complexes, e.g., porphyrins,[9] salens,[10] 1,4,7-triazacyclononane [11,12] derived catalysts, and iron tetradentate ligand complexes.[13] Catalytic systems based on different metals such as cobalt,[14] molybdenum,[15−17] vanadium,[17] tungsten,[18] manganese[19,20] rhenium,[21] and titanium[22] have also been reported for the epoxidation of a wide range of alkenes. The existing epoxidation processes, especially in the case of propylene oxide, are not environmentally friendly or give rise to significant amounts of byproducts.[4] Thus, new epoxidation procedures that are safer or more highly selective toward the epoxides would be industrially attractive.

Manganese oxides have great potential as selective heterogeneous catalysts, adsorbents, and battery materials.[23] They have been used for a wide range of industrial catalytic applications, e.g., ozone decomposition,[24] photocatalytic oxidation of organic pollutants,[25] nitric oxide reduction,[26−33] selective oxidations of

† Department of Chemistry, University of Connecticut.
‡ Department of Chemical Engineering, University of Connecticut.
§ Institute of Materials Sciences, University of Connecticut.
|| Department of Pharmacology, University of Connecticut Health Center.

(1) Paul, S. *Surface Coatings*; John Wiley & Sons Ltd: Chichester, U.K. 1996; pp 243−269.
(2) Ito, H.; Sasaki, H.; Tsuji, M.; Kohjiya, S. *Text. Res. J.* **1999**, *69*, 473−476.
(3) Nakajima, H.; Takase, S.; Terano, H.; Tanaka, H. *J. Antibiot.* **1997**, *50*, 96−99.
(4) Monnier, J. R. *Appl. Catal. A* **2001**, *221*, 73−91.
(5) Zuwei, X.; Ning, Z.; Yu, S.; Kunlan, L. *Science* **2001**, *292*, 1139−1141.
(6) Grigoropoulou, G.; Clark, J. H.; Elings, J. A. *Green Chem.* **2003**, *5*, 1−7.
(7) Bosing, M.; Noh, A.; Loose, I.; Krebs, B. *J. Am. Chem. Soc.* **1998**, *120*, 7252−7259.
(8) Linic, S.; Barteau, M. A. *J. Am. Chem. Soc.* **2003**, *125*, 4034−4035.
(9) Legemaat, G.; Drenth, W.; Schmidt, M.; Prescher, G.; Goor, G. *J. Mol. Catal. A* **1990**, *62*, 119−133.
(10) Schaus, S. E.; Brandes, B. D.; Larrow, J. F.; Tokunaga, M.; Hansen, K. B.; Gould, A. E.; Furrow, M. E.; Jacobsen, E. N. *J. Am. Chem. Soc.* **2002**, *124*, 1307−1315.
(11) Grenz, A.; Ceccarelli, S.; Bolm, C. *Chem. Commun.* **2001**, *18*, 1726−1727.
(12) Koek, J. H.; Kohlen, E. W. M. J.; Russell, S. W.; Van der Wolf, L.; Ter Steeg, P. F.; Hellemons, J. C. *Inorg. Chim. Acta* **1999**, *295*, 189−199.
(13) White, M. C.; Doyle, A. G.; Jacobsen, E. N. *J. Am. Chem. Soc.* **2001**, *123*, 7194−7195.
(14) Ikeno, T.; Iwakura, I.; Yamada, T. *J. Am. Chem. Soc.* **2002**, *124*, 15152−15153.
(15) Mitchell, J. M.; Finney, N. S. *J. Am. Chem. Soc.* **2001**, *123*, 862−869.
(16) Deubel, D. V.; Sundermeyer, J.; Frenking, G. *J. Am. Chem. Soc.* **2000**, *122*, 10101−10108.
(17) Chong, A. O.; Sharpless, K. B. *J. Org. Chem.* **1977**, *42*, 1587−1590.
(18) Sels, B. F.; De Vos, D. E.; Jacobs, P. A. *J. Am. Chem. Soc.* **2001**, *123*, 8350−8359.
(19) Lane, B. S.; Vogt, M.; DeRose, V. J.; Burgess, K. *J. Am. Chem. Soc.* **2002**, *124*, 11946−11954.
(20) Lane, B. S.; Burgess, K. *J. Am. Chem. Soc.* **2001**, *123*, 2933−2934.
(21) Gansauer, A. *Angew. Chem., Int. Ed. Engl.* **1997**, *36*, 2591−2592.
(22) Zimmer, A.; Moenter, D.; Reschetilowski, W. *J. Appl. Electrochem.* **2003**, *33*, 933−937.
(23) Brock, S. L.; Sanabria, M.; Nair, J.; Suib, S. L.; Ressler, T. *J. Phys. Chem. B* **2001**, *105*, 5404−5410.
(24) Radhakrishnan, R.; Oyama, S. T. *J. Catal.* **2001**, *199*, 282−290.
(25) Chen, J.; Lin, J. C.; Purohit, V.; Cutlip, M. B.; Suib, S. L. *Catal. Today* **1997**, *33*, 205−214.
(26) Qi, G.; Yang, R. T. *Appl. Catal. B* **2003**, *44*, 217−225.
(27) Kijlstra, W. S.; Brands, D. S.; Smit, H. I.; Poels, E. K.; Bliek, A. *J. Catal.* **1997**, *171*, 219−230.
(28) Kijlstra, W. S.; Brands, D. S.; Poels, E. K.; Bliek, A. *J. Catal.* **1997**, *171*, 208−218.
(29) Yamashita, T.; Vannice, A. *J. Catal.* **1996**, *163*, 158−168.
(30) Kijlstra, W. S.; Daamen, J. C. M. L.; Van de Graaf, J. M.; Van der Linden, B.; Poels, E. K.; Bliek, A. *Appl. Catal. B* **1996**, *7*, 337−357.

10.1021/ja048940x CCC: $27.50

carbon monoxide,[34] cyclohexane,[35,36] ethylbenzene,[37] ethanol[38] and 2-propanol,[39,40] decomposition of hydrogen peroxide,[41] hydrogenolysis of cyclopropane, and oligomerization of methane.[42] Porous manganese oxides either are amorphous or else crystallize as tunnel-structured materials (octahedral molecular sieves, OMS) or layered materials (octahedral layered phases, OL).[23,43] Correlations between the porosity of these materials and catalytic activity and selectivity have been found.[42,44] We recently have explored materials combining proteins with octahedral layered (OL-1) manganese oxide nanoparticles to make electroactive films and macroscopic helixes with catalytic activity.[45]

Layer-by-layer electrostatic assembly is a method of ultrathin film growth based on the alternate adsorption of oppositely charged polyions.[46] The key feature of this method is excessive surface adsorption at every stage of the polycation/polyanion assembly that leads to recharging of the outermost surface at every step of film formation. The layer-by-layer technique can include polyions, DNA, proteins,[47] viruses,[48] and charged nanoparticles.[49] This technique has been suitable for the construction of electronic, electro-optic, and charge storage devices, sensors, biocompatible films, and bioreactors.[50]

Enzyme/polyion films grown layer-by-layer have been used to catalyze organohalide reductions as well as epoxidation of styrene derivatives.[51,52] Lvov et al. constructed films of OL-1 nanoparticles with polycations and the protein myoglobin (Mb).[45a] Films made with nanoparticles involve three-dimensional film architecture with growth perpendicular to the solid support resulting in a porous structure. Because Mb was electrochemically and catalytically active in the protein/nanoparticle assemblies, these films could be used in electrochemical bioreactors. Our preliminary results showed that protein/OL-1 nanoparticle films catalyzed reduction of oxygen to form hydrogen peroxide, which in turn reacts with the film to form catalytic species that are capable of transferring oxygen to styrene. To our surprise, we found that both OL-1 nanoparticles and myoglobin are active for electrochemical catalysis of styrene epoxidation and may act by independent pathways.[45b]

In this paper, we report that in the presence of ~100 mM hydrogen peroxide and oxygen, OL-1 nanoparticles in films (without proteins) are excellent epoxidation catalysts. Synthetic, electrochemical, and ^{18}O labeling results were used to propose a pathway for styrene epoxidation by OL-1 manganese oxide nanoparticles.

Experimental Section

Chemicals. A colloidal solution of manganese oxide (OL-1) containing 0.01 M tetramethylammonium (TMA) permanganate was prepared according to published procedures.[23,43,48] Sodium poly(styrenesulfonate) (PSS, MW 70 000), poly(dimethyldiallylammonium chloride) (PDDA), catalase, and superoxide dismutase were from Aldrich. Hydrogen peroxide (30%) was from J. T. Baker. Water was purified by a Hydro Nanopure system to a specific resistance > 15 MΩ cm^{-2}. $^{18}O_2$ (99%, ^{18}O) and $H_2{}^{18}O_2$ were from Icon Isotopes.

Preparation of Films. Alternate adsorption onto solid substrates from aqueous solutions of PDDA (2 mg/mL, pH 12), PSS (3 mg/mL), and OL-1 nanoparticles (0.01 M, diameter ≈ 40 nm) was used as described previously.[45] Immersion time used for the adsorption was 15 min, and surfaces were rinsed with water between adsorption steps to remove weakly adsorbed molecules.

For QCM experiments, silver-coated quartz crystals were pretreated to generate a silver oxide layer (negatively charged). This pretreatment consisted in sonicating the silver coated quartz crystals in a mix of KOH/ethanol/water (1:60:39) for 30 s and then rinsing in water for 10 s. A positively charged polyelectrolyte layer such as PDDA was then adsorbed. Three layers (PDDA/PSS/PDDA) were typically adsorbed as a precursor film followed by alternate layers of OL-1 and PDDA

For cyclic voltammetry studies, multilayer films of PDDA and OL-1 were assembled onto basal plane pyrolytic graphite electrodes with the geometric area 0.16 cm^2 roughened by abrading on coarse emery paper (3M Crystal Bay). Three PSS/PDDA layers were adsorbed before the first layer of OL-1 was deposited to form a smooth bed for OL-1 adsorption. After the first layer of OL-1 was adsorbed, 9 PDDA/OL-1 layers were adsorbed to form a total of 10 layers of OL-1.

For catalytic oxidation of styrene, OL-1 films were prepared using a similar procedure in which three PSS/PDDA layers were adsorbed on both sides of 1.5 × 6 cm^2 carbon cloth prior to OL-1 layer. Only one layer of OL-1 was used for the oxidation experiments to minimize mass transport limitations.

Quartz Crystal Microbalance. A quartz crystal microbalance (QCM, USI System, Japan) was used to monitor the layer-by-layer growth. Frequency shifts were measured after carefully washing and drying the quartz crystal after each step of adsorption. The Sauerbrey equation gives a relationship between the frequency shift (ΔF) and the mass change in the absence of viscolelasticity differences.[46] The film mass per unit area M/A (g/cm^2) on a resonator of $A = 0.16 \pm 0.01$ cm^2 is given by eq 1, taking into account characteristics of the 9 MHz quartz

(31) Smirniotis, P. G.; Pena, D. A.; Uphade, B. S. *Angew. Chem., Int. Ed.* **2001**, *40*, 2479−2482.
(32) Chen, L.; Horiuchi, T.; Mori, T. *Appl. Catal. A* **2001**, *209*, 97−105.
(33) Yamashita, T.; Vannice, A. *J. Catal.* **1996**, *163*, 158−168.
(34) Xia, G. G.; Yin, Y. G.; Willis, W. S.; Wang, J. Y.; Suib, S. L. *J. Catal.* **1999**, *185*, 91−105.
(35) Xia, G. G.; Wang, J. Y.; Yin, Y. G.; Suib, S. L. In *Catalysis of Organic Reactions*; Herkes, F. E., Ed.; Marcel Dekker: New York, 1998; pp 615−620.
(36) Wang, J. Y.; Xia, G. G.; Yin, Y. G.; Suib, S. L. In *Catalysis of Organic Reactions*; Herkes, F. E., Ed.; Marcel Dekker: New York, 1998; pp 621−626.
(37) Vileno, E.; Zhou, H.; Zhang, Q.; Suib, S. L.; Corbin, D. R.; Koch, T. A. *J. Catal.* **1999**, *187*, 285−297.
(38) Zhou, H.; Wang, J. Y.; Chen, X.; O'Young, C. L.; Suib, S. L. *Microporous Mesoporous Mater.* **1998**, *21*, 315−324.
(39) Chen, X.; Shen, Y. F.; Suib, S. L.; O'Young, C. L. *J. Catal.* **2001**, *197*, 292−302.
(40) Cao, H.; Suib, S. L. *J. Am. Chem. Soc.* **1994**, *116*, 5334−5342.
(41) Zhou, H.; Shen, Y. F.; Wang, J. Y.; Chen, X.; O'Young, C. L.; Suib, S. L. *J. Catal.* **1998**, *176*, 321−328.
(42) Suib, S. L. *Chem. Innovation* **2000**, *30*, 27−33.
(43) Giraldo, O.; Durand, J. P.; Ramanan, H.; Laubernds, K.; Suib, S. L.; Tsapatsis, M.; Brock, S. L.; Marquez, M. *Angew. Chem., Int. Ed.* **2003**, *42*, 2905−2909.
(44) Giraldo, O.; Brock, S. L.; Willis, W. S.; Marquez, M.; Suib, S. L.; Ching, S. *J. Am. Chem. Soc.* **2000**, *122*, 9330−9331.
(45) (a) Lvov, Y.; Munge, B.; Giraldo, O.; Ichinose, I.; Suib, S. L.; Rusling, J. F. *Langmuir* **2000**, *16*, 8850−8857. (b) Espinal, L. M.S. Thesis, University of Connecticut, Storrs, CT, 2001. (c) Gao, Q.; Suib, S. L.; Rusling, J. F. *J. Chem. Soc., Chem. Commun.* **2002**, 2254−2255.
(46) (a) Lvov, Y.; Möhwald, H., Eds. *Protein Architecture: Interfacing Molecular Assemblies and Immobilization Biotechnology*;, Marcel Dekker: New York, 2000; pp 125−167. (b) Lvov, Y. In *Handbook Of Surfaces And Interfaces Of Materials, Vol. 3. Nanostructured Materials, Micelles and Colloids*; Nalwa, R. W., Ed.; Academic Press: San Diego, CA, 2001; pp 170−189. (c) Rusling, J. F. In *Protein Architecture: Interfacing Molecular Assemblies and Immobilization Biotechnology*; Lvov, Y., Möhwald, H., Eds. Marcel Dekker: New York, 2000; pp 337−354. (d) Rusling, J. F.; Zhang, Z. In *Handbook Of Surfaces And Interfaces Of Materials, Vol. 5. Biomolecules, Biointerfaces, And Applications*; Nalwa, R. W., Ed.; Academic Press: San Diego, CA, 2001; pp 33−71.
(47) Sano, M.; Lvov, Y.; Kunitake, T. *Annu. Rev. Mater. Sci.* **1996**, *26*, 153−187.
(48) Lvov, Y.; Haas, H.; Decher, G.; Moehwald, H.; Mikhailov, A.; Mtchedlishvily, B.; Morgunova, E.; Vainshtein, B. *Langmuir* **1994**, *10*, 4232−4236.
(49) Kotov, N.; Dekany, I.; Fendler, J. H. *J. Phys. Chem.* **1995**, *99*, 13065−13069.
(50) Hua, F.; Cui, T.; Lvov, Y. *Langmuir* **2002**, *18*, 6712−6715.
(51) Zu, X.; Lu, Z.; Zhang, Z.; Schenkman, J. B.; Rusling, J. F. *Langmuir* **1999**, *15*, 7372−7377.
(52) Rusling, J. F.; Zhang, Z. In *Handbook of Surfaces and Interfaces of Materials, Vol 5, Biomolecules, Biointerfaces and Applications*; Nalwa, H. S., Ed.; Academic Press: San Diego, CA, 2001; pp 33−71.

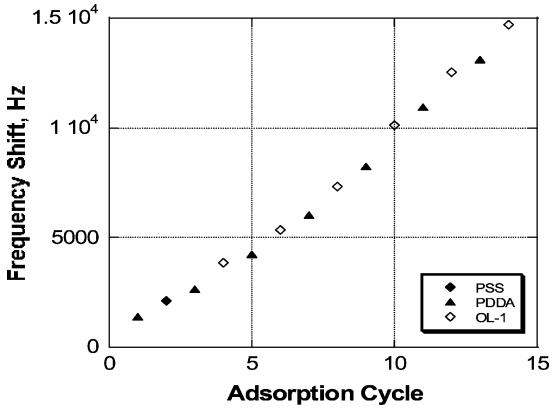

Figure 1. QCM frequency shifts for films assembled from OL-1 nanoparticles (0.01 M) and PDDA (2 mg/mL) on a bed of PDDA/PSS/PDDA silver resonators. Silver-coated quartz crystals were pretreated, as explained in the Experimental Section, to generate a negatively charged layer on top of which PDDA was adsorbed. Three layers (PDDA/PSS/PDDA) were adsorbed as a precursor film, followed by alternate layers of OL-1 and PDDA. Frequency shifts were measured after carefully washing and drying the quartz crystal after each step of adsorption. (Negative shift is upward.)

resonators. The nominal thickness of a dry film may be estimated taking into account the film density[53] by eq 2 which relates frequency shift (ΔF) and film thickness (d) of an adsorbed film on both sides of the electrode. X-ray reflectivity measurements and scanning electron microscopy of cross-section images were used to confirm these calculations.[45a,46]

$$\frac{M}{A}\,(\mathrm{g/cm^2}) = \frac{\Delta F\ (\mathrm{Hz})}{-1.83 \times 10^8} \tag{1}$$

$$d\ (\mathrm{nm}) \approx -(0.016 \pm 0.002)\Delta F\ (\mathrm{Hz}) \tag{2}$$

Electrochemistry. Voltammetry was done as described previously[45a] at 22 ± 2 °C. The cell for electrolysis employed a saturated calomel reference electrode (SCE), a carbon rod counter electrode, and a carbon cloth (National Electrical Carbon Corp., 1.5 × 6 cm^2) working electrode. The counter electrode was separated from the reaction solution by a saturated KCl agar bridge. Electrochemical oxidation of styrene was carried out in 10 mL of Tris buffer pH 7.4 saturated with styrene (~10 mM), usually at −0.60 V vs SCE. The cell was saturated with oxygen, and temperature was controlled at 4 °C to minimize loss of reactants and products under gas input conditions. Samples were extracted after 1 h of reaction with hexane and analyzed by GC by a previously described method.[51]

Results

Film Assembly. Film growth was monitored by frequency changes measured with a quartz crystal microbalance (QCM). The first three steps represent a polyion bed of PDDA/PSS/PDDA on the quartz crystal. Subsequent steps represent $(\text{OL-1/PDDA})_n$ layers (Figure 1). The data for the $(\text{OL-1/PDDA})_n$ films suggest a reproducible film growth process. ΔF was 1500 Hz for OL-1 adsorption steps, with a smaller step of 650 Hz for each PDDA layer. The growth of OL-1/PDDA films proceeded with a regular increase in mass in which each layer of OL-1 added 8.3 μg/cm^2 and PDDA added 3.6 μg/cm^2, based on eq 1. The corresponding nominal average thicknesses (from eq 2) for the OL-1 and PDDA layers were 24 ± 3 nm and 10 ± 1 nm, respectively. These results demonstrate the reproducibility of layer and film formation and are similar to those reported previously.[45a]

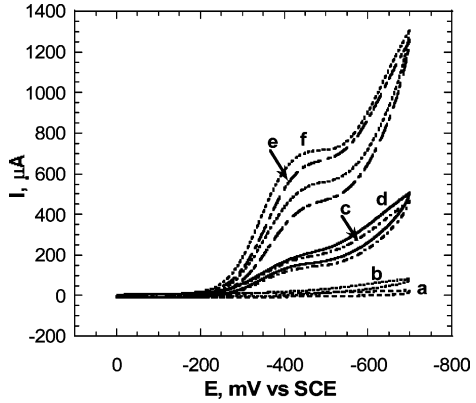

Figure 2. Cyclic voltammograms at 0.05 V·s^{-1} in pH 5.5 buffer for OL-1 film at different conditions. OL-1 film: PG-$(\text{PSS/PDDA})_3$/OL-1/$(\text{PDDA/OL-1})_9$; 10 layers of OL-1 in total were assembled onto basal plane pyrolytic graphite electrodes with the geometric area 0.16 cm^2. (a) No O_2/no H_2O_2, (b) O_2/no H_2O_2 (reduction of oxygen), (c) no O_2/10 mM H_2O_2, (d) O_2/10 mM H_2O_2, (e) no O_2/100 mM H_2O_2, and (f) O_2/100 mM H_2O_2.

Cyclic Voltammetry. OL-1/PDDA films were evaluated by cyclic voltammetry in buffers of 20 mM acetate (pH 5.5). Cyclic voltammograms of 10-layer OL-1 films in the absence of oxygen showed no electroactivity in the 0 to −0.7 V potential range (Figure 2a). However, the films showed a small increase in current in the presence of O_2 at −0.6 V vs SCE (Figure 2b) due to the reduction of oxygen. These films also showed a large reduction peak in the presence of H_2O_2 at potentials of −0.35 V vs SCE (Figures 2c−f). Figure 3 shows that control polyion films without OL-1 gave no evidence for reduction of O_2 or H_2O_2. Results indicate that both OL-1 and H_2O_2 have to be present for the reduction reactions to occur efficiently, and the data suggest the electrochemical catalytic reduction of H_2O_2 by OL-1. Similar results were obtained at pH 7.4.

Figure 4 shows cyclic voltammograms of OL-1 films under O_2 and 100 mM H_2O_2 with and without styrene. The presence of styrene does not seem to affect the behavior of these films in cyclic voltammetry. Cyclic voltammetry only provides information about the capability of these films to reduce oxygen and H_2O_2. Thus, to study the epoxidation of styrene, electrolysis and product analysis were employed.[52]

Styrene Epoxidation. Electrolysis experiments were done at potentials where the film reduces oxygen and hydrogen peroxide. It appears that this process produced activated OL-1, which then epoxidizes styrene to styrene oxide. Products were measured by gas chromatography. Chemical reactions with no applied voltage were also studied. Results from incubation of styrene with OL-1 films, at conditions appropriate for epoxidation, yielded styrene oxide and benzaldehyde as major products. Previous work using iron heme proteins as catalysts reported noncatalytic conversion of styrene to benzaldehyde by hydrogen peroxide.[51]

Table 1 summarizes results from the epoxidation of styrene under different conditions. In electrolysis experiments, at a constant applied potential of −0.6 V vs SCE, OL-1 in the presence of O_2 produced 0.09 μmol of styrene oxide (Table 1, entry 1), which indicates that OL-1 is able to oxidize styrene. The applied voltage is on the plateau of the catalytic H_2O_2 reduction wave in CV. The 6 mM concentration of H_2O_2 found

(53) Lvov, Y.; Ariga, K.; Ichinose, I.; Kunitake, T. *J. Am. Chem. Soc.* **1995**, *117*, 6117−6123.

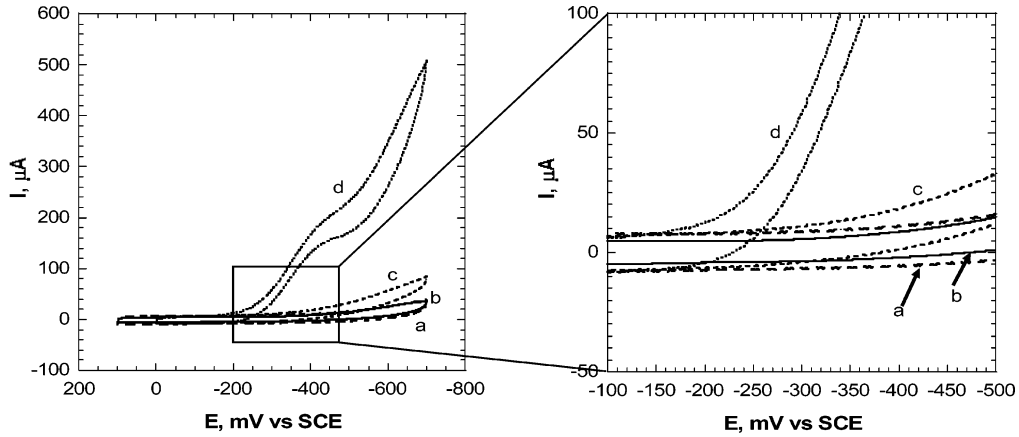

Figure 3. Cyclic voltammograms at 0.05 V·s^{-1} in pH 5.5 buffer. Polyion film: PG-(PSS/PDDA)$_3$. OL-1 film: PG-(PSS/PDDA)$_3$/OL-1/(PDDA/OL-1)$_9$. Multilayer films were assembled onto basal plane pyrolytic graphite electrodes with the geometric area 0.16 cm^2. (a) polyion film, O_2; (b) polyion film, O_2 /10 mM H_2O_2; (c) OL-1 film, O_2; and (d) OL-1 film, O_2/10 mM H_2O_2. (High sensitivity inset on right.)

Table 1. Oxidation of Styrene by OL-1 Film at 4° C[a] for 1 h

entry	film	O_2[b]	$E_{applied}$[c] (V vs SCE)	$[H_2O_2]_i$[d] added (mM)	styrene oxide[e] (μmol)	benzaldehyde[e] (μmol)	turnover rate[f] (h^{-1})	$[H_2O_2]_f$[g] found (mM)
1	OL-1[h]	yes	−0.6	0	0.09	0.06	0.05	6.0
2	OL-1	no	−0.6	0	0	0.01	0	0
3	OL-1 (+ catalase)[i]	yes	−0.6	0	0	0.01	0	0
4	PDDA (no OL-1)[j]	yes	−0.6	0	0.01	0.01		1.0
5	OL-1	yes		100	0.11	0.07	0.06	100
6	OL-1	no		100	0.07	0.03	0.04	100
7	PDDA (no OL-1)	yes		100	0.01	0.01		100
8	OL-1	yes	−0.6	100	5.20	0.05	3.0	100
9	OL-1	no	−0.6	100	0.39	0.05	0.2	100
10	OL-1 (+ superoxide dismutase)[k]	yes	−0.6	100	5.22	0.05	3.0	100
11	OL-1	yes	−0.45	0	0	0.01	0	1.6
12	OL-1	no	−0.45	100	0.36	0.01	0.2	100
13	OL-1	yes	−0.45	100	1.46	0.19	0.9	100

[a] All reactions were in pH 7.4 buffer (50 mM Tris + 50 mM NaCl) saturated with styrene (~10 mM). Mixing was performed using a magnetic stir bar. Temperature was controlled with a circulating water bath. Time of reaction: 1 h. All results were averaged for three or more reactions in 10 mL of solution. Reproducibility was ±20%. Electrode surface area used was 9 cm^2 (1.5 × 6 cm^2). [b] Yes/no: presence/absence of oxygen during the reaction. Oxygen flow rate used was 35 mL/min. [c] $E_{applied}$: constant potential applied. [d] $[H_2O_2]_i$: initial hydrogen peroxide concentration used. [e] GC-FID was used for the product analysis. The average retention time was 6.54 min for styrene oxide and 4.67 min for benzaldehyde. The total charge was 60 C, and the current efficiency, 2.5%. [f] Turnover rate (h^{-1}) = (moles of product)(moles of catalyst)$^{-1}$(time)$^{-1}$. Amounts of catalyst (OL-1) in films were calculated from QCM estimates of μg per cm^2 electrode area for OL-1 layer. [g] $[H_2O_2]_f$: final hydrogen peroxide concentration determined with an error margin of ±15% using Quantofix Peroxide 100 test sticks (Macherey-Nagel GmbH & Co., Germany). [h] OL-1: film with OL-1 as outer layer deposited onto polyion bed, (PSS/PDDA)$_3$−OL-1. [i] 3000 units catalase added. [j] PDDA: polyion film with PDDA as outer layer, (PSS/PDDA)$_3$. [k] 3000 units of superoxide dismutase added.

at the end of the reaction showed that the systems reduced O_2 to H_2O_2. Other electrolysis experiments were performed with OL-1 films in the absence of O_2 to prevent H_2O_2 formation (Table 1, entry 2). These experiments gave virtually no styrene oxide indicating that H_2O_2 is required for the epoxidation of styrene by OL-1. This result was confirmed with electrolysis experiments in which the enzyme catalase was added to rapidly destroy the H_2O_2 that was formed (Table 1, entry 3).[51] Results from these experiments gave no styrene oxide, showing once again that H_2O_2 is necessary for the epoxidation. Electrolysis in the absence of OL-1 (PDDA film) under oxygen conditions (Table 1, entry 4) produced 1 mM hydrogen peroxide but gave negligible amounts of styrene oxide supporting the important catalytic role that OL-1 plays in the epoxidation of styrene. Electrolysis experiments performed without O_2 and in the absence of OL-1 resulted in no products.

In electrolysis, oxygen is reduced at the electrode to form H_2O_2, which in turn may react chemically/electrochemically with OL-1 to form an active species that transfers oxygen to the olefinic bond of styrene. Since hydrogen peroxide is essential for styrene oxide formation, experiments were also done after adding additional hydrogen peroxide without any potential applied. In these chemical reactions, hydrogen peroxide con-

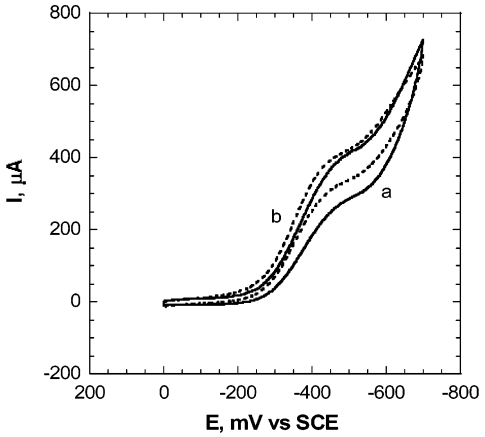

Figure 4. Cyclic voltammograms at 0.05 V·s^{-1} in pH 5.5 buffer for OL-1 film at different conditions. OL-1 film: PG-(PSS/PDDA)$_3$/OL-1/(PDDA/OL-1)$_9$; 10 layers of OL-1 in total were assembled onto basal plane pyrolytic graphite electrodes with the geometric area 0.16 cm^2. (a) O_2/100 mM H_2O_2 and (b) O_2/100 mM H_2O_2/saturate styrene.

centration also played an important role. Reactions with added amounts of 10 mM and 20 mM H_2O_2 produced no styrene oxide. Results from chemical reactions in which 100 mM H_2O_2 was directly added to the reaction mixture are shown in Table 1 (entries 5−7). The amounts of styrene oxide produced in these experiments were 0.11 μmol of styrene oxide in the presence of oxygen (Table 1, entry 5) and smaller amounts (0.07 μmol) in the absence of oxygen (Table 1, entry 6). These results confirmed that hydrogen peroxide is an essential component for the activation of OL-1 and can provide turnover even in the absence of electrolysis. Chemical reactions without OL-1 (PDDA film) in the presence of O_2 gave no styrene oxide (Table 1, entry 7). Control experiments with OL-1 film in the absence of both O_2 and H_2O_2 gave no styrene oxide.

Electrolysis combined with 100 mM H_2O_2 for OL-1 films in oxygen environments gave dramatically improved turnover (Table 1, entry 8). The amount of styrene oxide obtained from this experiment was 5.2 μmol of styrene oxide. In the absence of O_2, 0.39 μmol were found (Table 1, entry 9). We conclude that both O_2 and H_2O_2 play an important role in the epoxidation process on OL-1-coated electrodes.

It is possible that oxidant species such as superoxide anions could be formed during this reaction. However, the addition of superoxide dismutase, an enzyme that destroys superoxide anion,[54] did not affect the yields typically obtained (~5.2 μmol) under our conditions (Table 1, entry 10).

OL-1 films showed a steady-state catalytic reduction wave at $E_{1/2}$ of −0.35 V vs SCE in cyclic voltammetry in the presence of H_2O_2 (Figure 2c), which increased in the presence of oxygen and at larger H_2O_2 concentrations (Figures 2d−f). This electron transfer process was not observed when electrodes coated only with polyions were used, which suggests that this electron-transfer reaction may be involved in the epoxidation of styrene, since the control polyion electrode without OL-1 does not produce styrene oxide (Table 1, entries 4 and 7). Thus, it was important to check if the reduction peak observed in CV from Figure 2 (at −0.35 V vs SCE) was due to a reaction involved in the epoxidation mechanism, since films without OL-1 did not show this peak under the same conditions.

Electrolyses with OL-1 films at −0.45 V vs SCE in the presence of O_2 but with no H_2O_2 added, resulted in minimal products (Table 1, entry 11). In addition, the concentration of H_2O_2 measured at the end of the electrolysis at −0.45 V vs SCE (1.6 mM) was smaller compared to that obtained at −0.6 V vs SCE (6 mM). The amounts of styrene oxide obtained were negligible at −0.45 V vs SCE and 0.09 μmol at −0.6 V vs SCE. Electrolysis experiments were also performed at −0.45 V vs SCE in the presence of 100 mM H_2O_2 and in the absence of O_2 produced 0.36 μmol of styrene oxide (Table 1, entry 12), which is comparable with the styrene oxide amount formed in electrolysis at −0.6 V vs SCE at the same conditions. For electrolysis at −0.45 V vs SCE in the presence of both H_2O_2 (100 mM) and O_2 (Table 1, entry 13), the amount of styrene oxide obtained was almost 13 times larger (1.46 μmol) than that obtained from chemical reactions (0.11 μmol). Electrolyses at −0.6 V vs SCE at the same conditions gave 50 times more styrene oxide (5.2 μmol) compared to the amounts obtained in chemical reactions (0.11 μmol). These results indicate that the electron-transfer reaction observed by CV at −0.35 V vs SCE is part of the epoxidation mechanism and is definitively voltage dependent. The data obtained from synthetic experiments at lower applied potentials also confirm that the epoxidation reaction is dependent on the oxygen and hydrogen peroxide concentrations.

Table 2. Oxidation of Styrene by OL-1 Film [a] at 4°C[b] Using Electrolysis in the Presence of $^{18}O_2$ and/or $H_2{}^{18}O_2$

experimental conditions[c]	$[H_2O_2]$ [d] (mM)	O_2 flow rate (mL/min)	$S^{16}O$ [f] (%)	$S^{18}O$ [f] (%)	total SO [g] (μmol)
BE[e] + $^{18}O_2$	0	3	76	24	0.06
BE[e] + $H_2{}^{18}O_2$ + $^{16}O_2$	14	35	34	66	1.15
BE[e] + $H_2{}^{18}O_2$ + $^{18}O_2$	14	3	0	100	0.53
BE[e] + $H_2{}^{16}O_2$ + $^{18}O_2$	140	3	100	0	6.45

[a] OL-1: film with OL-1 as outer layer deposited onto polyion bed, $(PSS/PDDA)_3$−OL-1. [b] Temperature was controlled with a circulating water bath. [c] All reactions were in pH 7.4 buffer (50 mM Tris + 50 mM NaCl). Time of reaction: 1 h. All results were averaged for three or more reactions in 10 mL of solution. Reproducibility was ±20%. [d] $[H_2O_2]$: initial hydrogen peroxide concentration used. [e] BE: bulk electrolysis experiments performed at a constant applied potential of −0.6 V. [f] GC-FID was used for the product analysis. [g] Total SO: amount of $S^{16}O$ + $S^{18}O$ produced. The average retention time was 6.54 min for styrene oxide and 4.67 min for benzaldehyde. GC−MS was used for the detection of labeled and nonlabeled styrene oxide.

^{18}O-labeling. Electrolyses were also done with $^{18}O_2$ and $H_2{}^{18}O_2$ to understand the role of molecular oxygen, OL-1, H_2O_2, and the source of oxygen in the product. Table 2 shows the percentage of $S^{16}O$ and $S^{18}O$ obtained for all these experiments by GC−MS. Results show that 24% of ^{18}O is incorporated when $^{18}O_2$ is used and no H_2O_2 added. This $^{18}O_2$ incorporation increases to 66% when labeled $H_2{}^{18}O_2$ is used and $^{16}O_2$ is used. ^{18}O incorporation reaches almost 100% when both $H_2{}^{18}O_2$ and $^{18}O_2$ are used, which suggest that oxygen is not coming from the OL-1 lattice under these particular experimental conditions (14 mM $H_2{}^{18}O_2$ and $^{18}O_2$ flow rate of 3 mL/min). On the other hand, there was no ^{18}O incorporation when 140 mM $H_2{}^{16}O_2$ was used even though $^{18}O_2$ was bubbled into the reaction solution at 3 mL/min. Results from these labeling experiments confirm the important contribution of H_2O_2 in the mechanism of epoxidation by OL-1. Amounts of styrene oxide produced confirm the reaction rate dependence on O_2 and H_2O_2.

Discussion

QCM results (Figure 1) showed that the layer-by-layer method was successful for making stable films of OL-1 nanoparticles in alternation with PDDA. Lvov found a similar OL-1/PDDA ratio (2.1−2.4) in thickness for these nanoparticle−polyion assemblies and obtained a bilayer thickness of 27 nm, 18.4 nm for OL-1 and 8.6 nm for PDDA layers, which gives an OL-1/PDDA ratio of 2.1. We obtained a bilayer thickness of 34 nm, 24 nm for OL-1 and 10 nm for PDDA layers, which gives an OL-1/PDDA ratio of 2.4.

CV showed that OL-1 films reduce oxygen to hydrogen peroxide, which catalyzes the epoxidation of styrene-to-styrene oxide. OL-1 films produced hydrogen peroxide as well as styrene oxide (Table 1). Oxygen was reduced to hydrogen peroxide, a known reaction for manganese oxides,[55] at a potential of −0.6 V vs SCE (Figure 2b). In the presence of H_2O_2, OL-1 films showed a reduction wave at −0.35 V vs SCE

(54) Ortiz de Montellano, P. R.; Catalano, C. E. *J. Biol. Chem.* **1985**, *260*, 9265−9271.

(55) Matsuki, K.; Kamada, H. *Electrochim. Acta* **1986**, *31*, 13−18.

Scheme 1. Suggested Pathway for Electrochemical Styrene Epoxidation by OL-1[a]

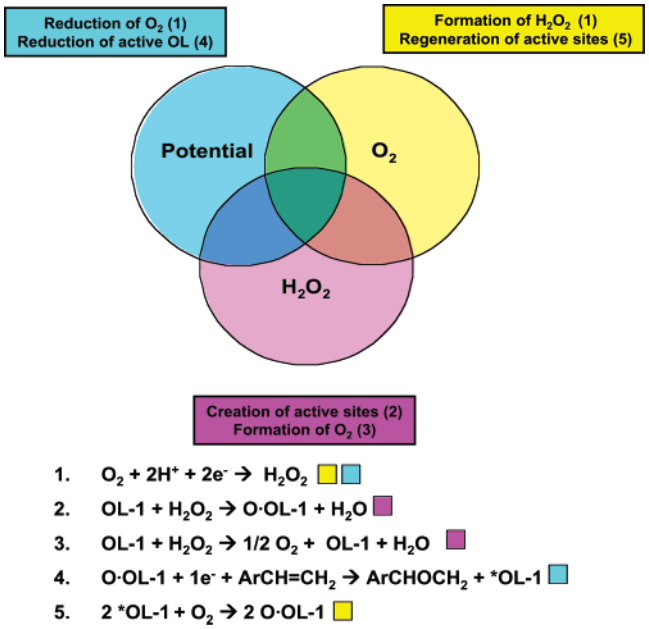

[a] *OL-1 **st**ands for OL-1 with vacant active sites and O·OL-1 for OL-1 with active oxidant sites. Colors beside steps in the pathway correlate to the items in the colored-coded circles.

(Figure 2c), which could be due to the reduction of an activated OL-1 species from the chemical reaction between H_2O_2 and OL-1. Manganese oxides particles undergo similar reactions.[41] Once the activated manganese oxide is reduced electrolytically, oxygen seems to play a very important role in regenerating active sites. Scheme 1 shows a representative pathway of all the reactions involved in this catalytic process: the electrode reduces both O_2[55] and activated OL-1 (O·OL-1), H_2O_2 activates OL-1 as well as produces O_2 from its decomposition on OL-1,[41] and O_2 forms H_2O_2 under electrolytic conditions[55] as well as regenerate the active sites[56] after activated OL-1 is reduced. The overall process results in reduction of H_2O_2 to H_2O.

From electrolysis in the presence of oxygen (Table 1, entry 1), 0.09 μmol of styrene oxide were produced, which indicates that the generated hydrogen peroxide (6 mM) assisted OL-1 in the oxidation of styrene at a relatively small turnover rate. This result was confirmed when catalase was added to destroy H_2O_2 in a similar experiment and gave no products (Table 1, entry 3). Results from chemical reactions or direct addition of H_2O_2 (100 mM) with no potential applied gave 0.11 μmol of styrene oxide (Table 1, entry 5), which proves that OL-1 can be activated by H_2O_2 alone to produce styrene oxide.

Addition of H_2O_2 to electrolysis mixtures in the presence of oxygen greatly improved the yields (Table 1, entry 8), which indicates that epoxidation efficiency depends critically on the H_2O_2 concentration. Similar trends were found when a potential of -0.45 V vs SCE was used (Table 1, entries 11−13). The yields for styrene oxide increased at this potential when H_2O_2 was added. However, these increments were lower at -0.45 V vs SCE compared to equivalent experiments at -0.6 V vs SCE, suggesting that the rate of epoxidation depends strongly on the applied potential as well. Electrolyses were performed in oxygen

Table 3. Source of the Oxygen in Styrene Oxidation by OL-1 Film[a] at 4 °C[b] Using Electrolysis in the Presence of O_2 and/or H_2O_2

experimental conditions[c]		O-incorporation (%)		
$[H_2O_2]$[d] (mM)	O_2 flow rate (mL/min)	H_2O_2	O_2	lattice-O
0	3	0	24	76
14	35	66	34	0
140	3	~100	0	0

[a] OL-1: film with OL-1 as outer layer deposited onto polyion bed, $(PSS/PDDA)_3$−OL-1. [b] Temperature was controlled with a circulating water bath. [c] All reactions were in pH 7.4 buffer (50 mM Tris + 50 mM NaCl). Time of reaction: 1 h. Potential applied: −0.6 V vs SCE. All results were averaged for three or more reactions in 10 mL of solution. Reproducibility was ±20%. [d] $[H_2O_2]$: initial hydrogen peroxide concentration used. [g] Data in this table were taken from data shown in Table 2.

environments in the presence of different added amounts of H_2O_2: 0, 14, and 100 mM H_2O_2 gave 0.09 (Table 1, entry 1), 1.15 (Table 2), and 5.20 (Table 1, entry 8) μmol of styrene oxide, respectively. These results confirm that the rate of epoxidation is H_2O_2 concentration dependent. Analogously, the O_2 concentration or O_2 flow rate also affects the rate of epoxidation. Electrolyses were performed in the presence of 14 mM H_2O_2 at different O_2 flow rates: 3 and 35 mL/min gave 0.53 and 1.15 μmol of styrene oxide, respectively (Table 2). Furthermore, as mentioned previously, the absence of oxygen always resulted in lower amounts of styrene oxide produced. Thus, the rate of epoxidation is O_2 concentration dependent as well.

In general, results agree with the pathway shown in Scheme 1: H_2O_2 needs to activate OL-1[41] (step 2), and then O·OL-1 is reduced when electrical potential is applied (step 4), transferring oxygen to styrene producing a manganese oxide with a vacant active site represented as *OL-1 which will then be regenerated to O·OL-1 by O_2. Step 4 represents the key oxygen transfer to the olefinic bond. The equation as written reflects the role of catalytic electrochemical activation and regeneration of the active site on the catalyst, although the details of this process are still under investigation. Scheme 1 also shows other roles of O_2, H_2O_2, and potential that indirectly participate in the reaction: O_2 can form H_2O_2 electrochemically (step 1); H_2O_2 can form O_2 after reacting with OL-1 (step 3).

Superoxide anion is ruled out as an oxidant in the epoxidation because the addition of superoxide dismutase did not influence the amounts of styrene oxide produced (Table 1, entry 10). Other oxidant species such as radicals, peroxy radicals, singlet oxygen, or peroxy anion could possibly be involved. Further experiments using scavengers of these species would be necessary to elucidate their role, if any. Data from the present work suggest that at least one of the oxidant species comes from H_2O_2, but this may also involve the MnO_2 nanoparticles.

The precedence of the oxygen transferred to styrene was determined from electrolysis experiments using $^{18}O_2$ and/or $H_2{}^{18}O_2$. Results indicate that the oxygen transferred to styrene comes from different sources: molecular oxygen, hydrogen peroxide, and/or lattice oxygen from OL-1[56] depending on the experimental conditions which include oxygen flow rate, hydrogen peroxide concentration, and constant potential applied (Table 3). When low O_2 flow rates are used in the absence of H_2O_2, the oxygen transferred to styrene comes from molecular oxygen as well as from the OL-1 lattice.[57,58] On the other hand, when O_2 is used in the presence of H_2O_2, there are two

(56) Makwana, V. D.; Son, Y. C.; Howell, A. R.; Suib, S. L. *J. Catal.* **2002**, *210*, 46−52.

tendencies: (1) if high concentrations of H_2O_2 are used in the presence of O_2, most of the oxygen transferred comes from H_2O_2, and (2) if low concentrations of H_2O_2 are used, the oxygen transferred comes from both O_2 and H_2O_2. Interestingly, oxygen does not come from the OL-1 lattice when there are both O_2 and H_2O_2 present.

Conclusions

OL-1 nanoparticle/polyion films on carbon electrodes electrochemically catalyze styrene epoxidation. The reaction pathway involves H_2O_2, O_2, and a reducing voltage. Oxygen incorporation to styrene takes place from three possible sources: molecular oxygen, hydrogen peroxide, and/or lattice oxygen from OL-1 depending on the constant potential applied and on the oxygen and hydrogen peroxide concentrations. A key step involves the activation of the catalyst by hydrogen peroxide. In this respect, the reaction has some similarity to hydrogen peroxide-activated oxidations catalyzed by iron heme enzymes such as peroxidases or cyt P450s.[59] Further work is underway to establish the generality of the epoxidation method and to develop experimental and reactor conditions leading to high yields.

Acknowledgment. This work was supported financially by the National Science Foundation under Grants No. CTS-9982854 and CTS-0335345 (J.F.R.) and the U.S. Department of Energy (S.L.S.).

Supporting Information Available: Mass spectra of products from styrene electrolyses done with $^{18}O_2$ and $H_2{}^{18}O_2$. This material is available free of charge via the Internet at http://pubs.acs.org.

JA048940X

(57) Yin, Y. G.; Xu, W. Q.; DeGuzman, R.; Suib, S. L.; O'Young, C. L. *Inorg. Chem.* **1994**, *33*, 4384−4389.
(58) Yin, Y. G.; Xu, W. Q.; Shen, Y. F.; Suib, S. L.; O'Young, C. L. *Chem. Mater.* **1994**, *6*, 1803−1808.
(59) (a) Everse, J.; Everse, K. E. In *Peroxidases in Chemistry and Biology*, *Vol. II*; Grisham, M. B., Ed.; CRC Press: Boca Raton, FL, 1991. (b) Schenkman, J. B.; Greim, H., Eds. *Cytochrome P450*; Springer-Verlag: Berlin, 1993.